

Compression of ultra-long microwave pulses using programmable microwave photonic phase filtering with > 100 complex-coefficient taps

Minhyup Song,^{1,2,*} Victor Torres-Company,^{1,3} Rui Wu,¹ Andrew J. Metcalf,¹ and Andrew M. Weiner^{1,4}

¹*School of Electrical and Computer Engineering, Purdue University, 465 Northwestern Avenue, West Lafayette, IN 47907-2035, USA*

²*Current address: Electronics and Telecommunication Research Institute, 218 Gajeongno, Yuseong-gu, Daejeon, 305-700, South Korea*

³*Current address: Microtechnology and Nanoscience department, Chalmers University of Technology, SE-412 96 Gothenburg, Sweden*

⁴*amw@purdue.edu*

**song55@purdue.edu*

Abstract: Microwave photonic filters with arbitrary phase response can be achieved by merging high-repetition-rate electro-optic frequency comb technology with line-by-line pulse shaping. When arranged in an interferometric configuration, the filter features a number of programmable complex-coefficient taps equal to the number of available comb lines. In this work, we use an ultrabroadband comb generator resulting in a microwave photonic phase filter with >100 complex-coefficient taps. We demonstrate the potential of this filter by performing programmable chirp control of ultrawideband waveforms that extend over long (>10 ns) temporal apertures. This work opens new possibilities for compensating realistic linear distortion impairments on ultrabroadband wireless signals spanning over dozens of nanosecond temporal apertures.

© 2014 Optical Society of America

OCIS codes: (060.5625) Radio frequency photonics; (100.5090) Phase-only filters; (320.5520) Pulse compression; (320.5540) Pulse shaping; (320.6629) Supercontinuum generation; (320.7110) Ultrafast nonlinear optics.

References and links

1. J. P. Yao, "Microwave photonics," *J. Lightwave Technol.* **27**(3), 314–335 (2009).
2. J. Capmany, B. Ortega, and D. Pastor, "A tutorial on microwave photonic filters," *J. Lightwave Technol.* **24**(1), 201–229 (2006).
3. B. Ortega, J. L. Cruz, J. Capmany, M. V. Andres, and D. Pastor, "Variable delay line for phased-antenna based on a chirped fiber grating," *IEEE Trans. Microw. Theory Tech.* **48**(8), 1352–1360 (2000).
4. Y. Liu, J. Yang, and J. Yao, "Continuous true-time-delay beamforming for phased array antenna using a tunable chirped fiber grating delay line," *IEEE Photon. Technol. Lett.* **14**(8), 1172–1174 (2002).
5. D. B. Hunter, M. E. Parker, and J. L. Dexter, "Demonstration of a continuously variable true-time delay beamformer using a multichannel chirped fiber grating," *IEEE Trans. Microw. Theory Tech.* **54**(2), 861–867 (2006).
6. S. Xiao and A. M. Weiner, "Programmable photonic microwave filters with arbitrary ultra-wideband phase response," *IEEE Trans. Microw. Theory Tech.* **54**(11), 4002–4008 (2006).
7. J. G. Proakis, *Digital Communications*, 4th ed., (McGraw-Hill, 2001).
8. P. Tortoli, F. Guidi, and C. Atzeni, "Digital vs SAW matched filter implementation for radar pulse compression," *Proc. IEEE Ultrason. Symp.* **1**, 199–202 (1994).
9. J. D. McKinney and A. M. Weiner, "Compensation of the effects of antenna dispersion on UWB waveforms via optical pulse shaping techniques," *IEEE Trans. Microw. Theory Tech.* **54**(4), 1681–1686 (2006).
10. M. Bolea, J. Mora, B. Ortega, and J. Capmany, "Highly chirped single-bandpass microwave photonic filter with reconfiguration capabilities," *Opt. Express* **19**(5), 4566–4576 (2011).
11. M. Li, A. Malacarne, N. Belhadj, S. LaRochelle, J. Yao, and J. Azana, "Reconfigurable and single-shot chirped microwave pulse compression using a time-spectrum convolution system," postdeadline paper, IEEE Microwave Photonics Conference (2011).

12. E. Hamidi and A. M. Weiner, "Post-compensation of ultra-wideband antenna dispersion using microwave photonic phase filters and its applications to UWB systems," *IEEE Trans. Microw. Theory Tech.* **57**(4), 890–898 (2009).
13. E. Hamidi and A. M. Weiner, "Phase-only matched filtering ultrawideband arbitrary microwave waveforms via optical pulse shaping," *J. Lightwave Technol.* **26**(15), 2355–2363 (2008).
14. M. Sagues, A. Loayssa, and J. Capmany, "Multi-tap complex-coefficient incoherent microwave photonic filters based on stimulated Brillouin scattering," *IEEE Photon. Technol. Lett.* **19**(16), 1194–1196 (2007).
15. T. Mengual, B. Vidal, and J. Marti, "Continuously tunable photonic microwave filter based on a spatial light modulator," *Opt. Commun.* **281**(10), 2746–2749 (2008).
16. X. Yi, T. X. H. Huang, and R. A. Minasian, "Tunable and reconfigurable photonic signal processor with programmable all-optical complex coefficients," *IEEE Trans. Microw. Theory Tech.* **58**(11), 3088–3093 (2010).
17. Y. Dai and J. P. Yao, "Nonuniformly-spaced photonic microwave delayline filter," *Opt. Express* **16**(7), 4713–4718 (2008).
18. E. Hamidi, D. E. Leaird, and A. M. Weiner, "Tunable programmable microwave photonic filters based on an optical frequency comb," *IEEE Trans. Microw. Theory Tech.* **58**(11), 3269–3278 (2010).
19. M. Song, C. M. Long, R. Wu, D. Seo, D. E. Leaird, and A. M. Weiner, "Reconfigurable and tunable flat-top microwave photonic filters utilizing optical frequency comb," *IEEE Photon. Technol. Lett.* **23**(21), 1618–1620 (2011).
20. V. Torres-Company, J. Lancis, and P. Andrés, "Lossless equalization of frequency combs," *Opt. Lett.* **33**(16), 1822–1824 (2008).
21. Z. Jiang, D. S. Seo, D. E. Leaird, and A. M. Weiner, "Spectral line-by-line pulse shaping," *Opt. Lett.* **30**(12), 1557–1559 (2005).
22. M. Song, V. Torres-Company, A. J. Metcalf, and A. M. Weiner, "Multitap microwave photonic filters with programmable phase response via optical frequency comb shaping," *Opt. Lett.* **37**(5), 845–847 (2012).
23. V. Ataie, B. P.-P. Kuo, E. Myslivets, and S. Radic, "Generation of 1500-tone, 120 nm-wide ultraflat frequency comb by single CW source," postdeadline paper, Optical Fiber Communication Conference (OFC) (2013).
24. A. J. Metcalf, V. Torres-Company, D. E. Leaird, and A. M. Weiner, "High-Power Broadly Tunable Electro-Optic Frequency Comb Generator," *IEEE J. Sel. Top. Quantum Electron.* **19**(6), 231 (2013), doi:10.1109/JSTQE.2013.2268384.
25. C. B. Huang, S. G. Park, D. E. Leaird, and A. M. Weiner, "Nonlinearly broadened phase-modulated continuous-wave laser frequency combs characterized using DPSK decoding," *Opt. Express* **16**(4), 2520–2527 (2008).
26. C. Finot, B. Kibler, L. Provost, and S. Wabnitz, "Beneficial impact of wave-breaking for coherent continuum generation in normally dispersive nonlinear fibers," *J. Opt. Soc. Am. B* **25**(11), 1938–1948 (2008).
27. R. Wu, V. Torres-Company, D. E. Leaird, and A. M. Weiner, "Supercontinuum-based 10-GHz flat-topped Optical Frequency Comb Generation," *Opt. Express* **21**(5), 6045–6052 (2013).
28. A. M. Weiner, *Ultrafast Optics* (Wiley Interscience, 2009).

1. Introduction

Microwave photonic (MWP) techniques enhance the performance of ultrabroadband radio-frequency (RF) systems via the wideband and low-loss capability in optics [1]. This perspective offers attractive features unattainable with conventional electronics solutions such as insensitivity to electromagnetic interference, compatibility with optical fiber networks, easy tuning and programmability over an ultrabroad bandwidth [1]. One of the most promising applications in MWP is the implementation of microwave filters for high carrier frequency and wide bandwidth RF waveforms [2]. However, most of the research efforts in MWP filters (MWPFs) are focused on modifying the amplitude response, with the exception of exploiting linear spectral phase characteristics [3–5]. The synthesis of broadband filters with a user-defined quadratic or even higher-order nonlinear phase response is a much more challenging task [6]. This enables processing based on phase-only matched filtering, where the filter introduces the opposite of an electrical waveform's spectral phase to cancel the nonlinear phase components of the signal [7].

One of the most important practical issues of the filters is to get a large time-bandwidth product (TBWP) and operate over long temporal apertures, as required by the fields of modern radar systems [8] or compensation of antenna distortions [9]. In other words, the filter must manipulate the spectral components over the bandwidth of interest with very fine resolution. Recent research efforts for MWPFs with arbitrary spectral phase response have been implemented based on a microwave coherent filter using optical pulse shaping with hyperfine resolution [6]; amplitude modulation of a broadband optical source chirped by a nonlinear dispersive element and sliced by an interferometric system [10]; and a real-time

time-spectrum convolution system [11]. In [6], a programmable phase filter with 19 GHz bandwidth and a TBWP of ~ 32 was reported, which was applied for matched filtering of large TBWP ultrawide bandwidth waveforms [12,13]. Although the filter shows a relatively large TBWP, the temporal aperture is limited by the optical spectral resolution [12]. In [11], another interesting configuration based on a programmable optical spectral processor to shape a broadband multi-wavelength laser source was presented. Although it allows reconfigurable and single-shot chirped microwave pulse compression, the setup presents an unwanted response at baseband.

It is very difficult to achieve MWPFs with simultaneously large temporal apertures, bandwidth programmability, and bandpass central frequency tuning. This kind of flexibility can be met by realizing finite impulse response (FIR) filters with programmable complex coefficient taps. Such a degree of flexibility enables new signal processing applications in radar, ultrawideband communication, and arbitrary waveform generation [1]. In this direction, there have been several interesting proposals based, e.g., on stimulated Brillouin scattering [14], a phase spatial light modulator used in cross-polarized carrier-sideband geometry [15], a pulse shaper capable of resolving and applying different phases to optical carriers and sidebands [16], and non-uniform tap spacing [17]. However, these techniques were demonstrated only for a small number of taps, and few have reported operation over tens of taps.

Table 1. Comparison of Reconfigurable MWP Phase Filters

Scheme	Aperture (ns)	TBWP	Tunable	Programmable
Coherent pulse shaping ^a	~ 1.66	~ 32	No	Yes
Incoherent chirped source ^b	~ 15	~ 75	Yes	No
Time-Spectrum convolution ^c	~ 3.3	~ 4	No	Yes
Incoherent FIR comb-based ^d	~ 2	~ 10	Yes	Yes
This work ^e	~ 16	~ 34	Yes	Yes

FIR: Finite-Impulse Response; TBWP: Time-bandwidth product.

^a From [6]. MWPF with 600 MHz resolution over 19 GHz bandwidth.

^b From [10]. MWPF data inferred from Fig. 9(c).

^c From [11]. Data inferred from pulse compression example in Fig. 4(c).

^d From [22] MWPF data: 2 ns duration and 5 GHz bandwidth.

^e MWPF parameters achieved: 16 ns aperture and 2.1 GHz bandwidth.

In order to design MWPFs with a large number of complex taps, our group has recently adopted a dispersive delay-line configuration in an interferometric arrangement [18,19] with an electro-optic frequency comb (OFC) generator [20] as the single laser-fed multi-tap source. When combined with line-by-line pulse shaping, this solution provides the desired full programmability [21]. This setup also allows for a MWPF with programmable phase response, as demonstrated in [22]. Using this setup but a different ultrabroadband comb generator, here we show a MWPF with >160 complex-coefficient programmable taps. The filter is used to compress an ultra-complex waveform, with a time aperture longer than 10 ns and a TBWP spanning greater than 30, to its bandwidth-limited duration. The spectral resolution of the MWP filter is almost an order of magnitude better than our previous results [22] and, to the best of our knowledge, both the TBWP and the temporal aperture are the highest achieved in a programmable manner. The properties of various published MWP phase filters with respect to time aperture, TBWP, tuning capabilities and programmability are summarized in Table 1. We note that our filter has a clear advantage in both time aperture and TBWP compared to other programmable phase filters. We also note that our technique also could be easily scaled up by using combs with more lines, such as the one presented in [23].

2. Microwave phase filtering setup

2.1 Interferometric dispersive-delay-line microwave photonic filtering

The interferometric dispersive-delay-line MWP filter scheme that we follow in this work has been successfully demonstrated previously in [19, 22]. It uses a multi-carrier light source in a dispersive-delay-line configuration that provides an FIR filter with complex coefficient taps. The key difference compared to [19, 22] is that the electro-optic frequency comb generator is subject to substantial nonlinear spectral broadening, see below, which enables a substantial improvement in the filter's spectral resolution. In Fig. 1, an ultra-broadband optical frequency comb (OFC) is amplified with an erbium-doped fiber amplifier (EDFA), and the optical carriers are divided into two paths with a 50/50 optical splitter. The light through path 1 experiences optical single-sideband modulation with the carriers suppressed. This is achieved using a dual-drive Mach-Zehnder modulator biased at the quadrature point and excited by two copies of the RF signal to be filtered with 90 degree phase difference. The modulator output is connected to a periodic optical filter implemented by 10 Gb/s differential phase-shift keying demodulator (a delay imbalanced Mach-Zehnder interferometer) which has deep nulls in its transmission response with 10 GHz periodicity matched to the repetition-rate of the comb source. The nulls are tuned to remove the optical carriers, leaving the modulated sidebands only. Thus, the combination of the modulator with the periodic filter provides the desired carrier-suppressed single-sideband modulation. The portion of the OFC in path 2 undergoes spectral phase shaping of the individual comb lines by a commercial pulse shaper. The two interferometer paths are aligned in polarization, coupled back together, and passed through a dispersion compensating fiber (DCF) that has -1259.54 ps/nm chromatic dispersion at 1550 nm, which results in a delay difference of 96 ps between adjacent 10 GHz comb lines. Considering 160 taps, this provides a maximum temporal aperture of ~ 16 ns. After photodetection in a 22 GHz bandwidth photodiode, we measure the amplitude and the phase of the transfer function (S21 parameter) using a vector network analyzer (VNA). At the photodiode, the output electrical signal is physically composed by a sum of beat terms between each of the RF sidebands from path 1 and the nearest shaped comb line from path 2. In this way, optical amplitude and phase programming enables the full complex control of the output RF signal. When the shaper is programmed in phase-only mode, the electrical filter transfer function can be written as [19, 22]

$$H(\omega_{RF}) \propto \sum_n e_n^2 \exp[jnD\Delta\omega(\omega_{RF} + \tau/D) - j\Phi_n]. \quad (1)$$

where e_n^2 is the optical intensity of the n^{th} tap, D is the fiber dispersion (in ps^2), $\Delta\omega$ is the repetition frequency of the comb, $D\Delta\omega$ is the delay between two adjacent taps, τ is the relative delay between path 1 and 2 in Fig. 1, which allows for filter tuning, and Φ_n is the phase applied to the n^{th} comb line with the pulse shaper. This equation indicates that the central frequency of the filter is tunable and that complex coefficient filters can be attained with the aid of a programmable line-by-line pulse shaper. The more taps, the larger the filter's TBWP.

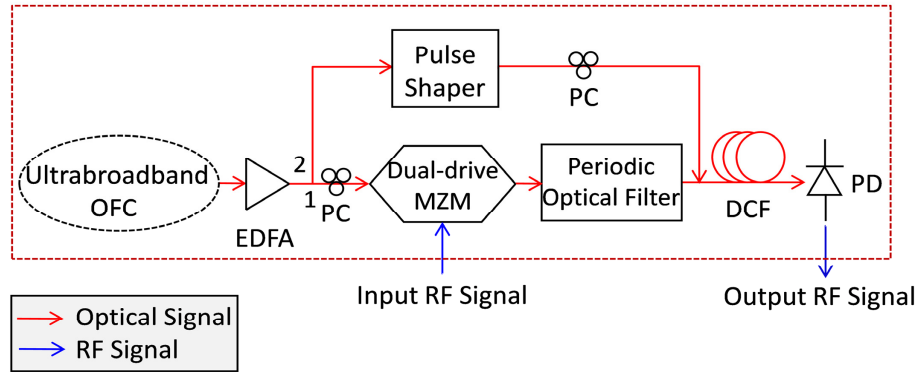


Fig. 1. Schematic diagram of the experimental setup for the complex-coefficient-tap MWP phase filter. MZM: Mach-Zehnder modulator; EDFA: erbium-doped fiber amplifier; DCF: dispersion compensating fiber; PD: photodetector; RF: radio-frequency.

2.2 Ultrabroadband comb generator

The details of our ultrabroadband OFC generator in Fig. 1 are shown in Fig. 2(a). A continuous-wave (CW) laser is sent through a series of three electro-optic phase modulators (PMs) and an intensity modulator (IM), all driven by a tunable RF oscillator working at 10 GHz. The DC bias on the IM is set to achieve a flat-top pulse. By aligning the cusp of the phase modulation from each PM with the peak of the flat-top pulse produced by the IM, a spectrum with ~60 lines and relatively flat profile is achieved (see Fig. 2(b)). The chirp from the phase-modulation stage can be approximately compressed with dispersive linear single-mode fiber. More details of the performance of this comb generator and the procedure to align the PMs and IM are provided in [24]. After pulse compression, we exploit nonlinear spectral broadening in an external highly nonlinear fiber (HNLF) in order to achieve more comb lines [25]. It is well known that a flattened supercontinuum source can be generated by pumping the HNLF in the normal dispersion regime with a Gaussian-shaped pulse (see e.g., [26,27]). We follow this approach and reshape the input flat-top comb into a Gaussian envelope with the aid of a commercial pulse shaper (Finisar Waveshaper 1000s). After polarization control, the Gaussian pulse was amplified up to 1.7 W with a high-power EDFA and connected to 100 meter of a HNLF with dispersion -1.88 ps/nm/km and nonlinear coefficient of 10 (W·km) $^{-1}$, as specified by the manufacturer. The resulting spectrum shows a power variation of 15 dB across 50 nm. A smooth portion of the spectrum at the output of the HNLF is selected using an optical bandpass filter (BPF) (8nm at -10 dB) as shown in Fig. 2(c), which also helps to suppress part of the ASE from the EDFA. The spectrum shows ~160 comb lines within 20 dB and a desirable bell-shaped apodization. This OFC will serve as the multi-wavelength light source for the MWPF, whose layout was presented in Fig. 1.

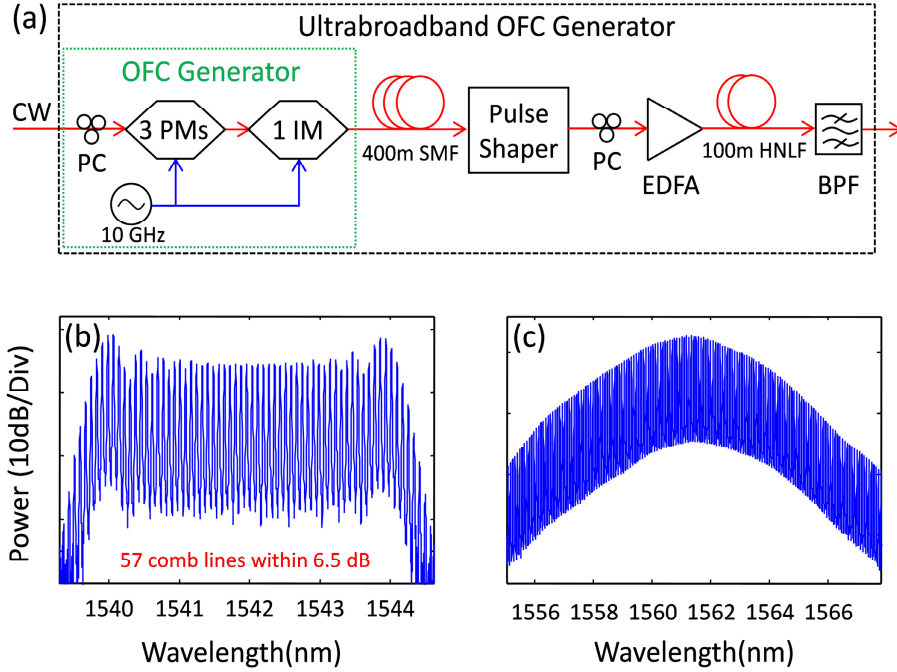


Fig. 2. (a) Schematic diagram of the experimental setup for the ultrabroadband OFC generator used as multi-wavelength comb source. CW: continuous-wave; PC: polarization controller; PM: phase modulator; IM: intensity modulator; SMF: single-mode fiber; HNLF: highly nonlinear fiber; BPF: bandpass filter. Measured optical power spectrum of (b) high power OFC generator and (c) smoothened and truncated ultrabroadband OFC.

2.3 Programmable chirp control

If we apply an optical quadratic phase ($\Phi_n = \beta n^2$) through the pulse shaper, the filter response function, Eq. (1), becomes

$$H(\omega_{RF}) \propto \sum_n e_n^2 \exp\left[jnD\Delta\omega\left(\tilde{\omega}_{RF} - \frac{\beta n}{D\Delta\omega}\right)\right] \quad (2)$$

where $\tilde{\omega}_{RF} (= \omega_{RF} + \tau/D)$ is the frequency offset from center of the filter passband, and the β parameter characterizes the applied quadratic phase. When the quadratic phase is sufficiently large, we write

$$\tilde{\omega}_{RF} = \frac{\beta n}{D\Delta\omega} \quad (3a)$$

or conversely

$$n = \frac{D\Delta\omega\tilde{\omega}_{RF}}{\beta}. \quad (3b)$$

By this we mean that the filter response around frequency $\tilde{\omega}_{RF}$ arises primarily from taps around tap n . The corresponding delay for tap n is simply expressed as $\tau_n = nD\Delta\omega$. Hence

$$\tau(\tilde{\omega}_{RF}) = \frac{(D\Delta\omega)^2}{\beta} \tilde{\omega}_{RF}. \quad (4)$$

Thus, within our large-phase approximation, the frequency-dependent delay is proportional to RF frequency. This corresponds to quadratic RF spectral phase, i.e., $\psi(\omega_{RF}) \sim \psi_2 \omega_{RF}^2/2$, where ψ_2 is the second-order spectral phase coefficient. The frequency dependent delay is then given by $\tau(\omega) = -\psi_2 \omega_{RF}$ [28]. As a result, the dispersion ($2\pi\psi_2$) within the bandpass (in ns/GHz) becomes

$$2\pi\psi_2 = -\frac{2\pi(D\Delta\omega)^2}{\beta}. \quad (5)$$

Figure 3 shows the measured amplitude and phase filter response when β equals to -0.017 . This value is chosen to maximize the ψ_2 parameter, according to a numerical analysis based on Eq. (1). In Fig. 3(a), the center frequency of the band-pass, controlled by applying linear spectral phase across the comb lines using a pulse shaper, is 2.6 GHz (this is equivalent to imposing a delay τ of 24.9 ps), and the bandwidth is ~ 2.1 GHz at the -10 dB level. The simulation (dashed), obtained from Eq. (2) using the measured comb shown in Fig. 2(c), is in close agreement with the measurement (solid). The smooth rolloff of the amplitude response reflects the Gaussian apodization of the optical power spectrum. Figure 3(b) shows the measured delay (solid) within the passband, obtained by differentiating the phase response measured by the VNA. As expected, it shows linear dispersion (i.e. quadratic spectral phase response) in the passband, and the chirp rate is 3.7 ns/GHz, as obtained by fitting to a straight line. It is in reasonable agreement with the approximate theoretical result (dotted) calculated using Eq. (5) (3.4 ns/GHz) and the simulated result (dashed) obtained from Eq. (2) using the actual comb spectrum and the programmed quadratic phase to the pulse shaper (3.5 ns/GHz). We note that the difference between measured and expected chirp rates may be attributed to phase errors in pulse shaper caused by limited spectral resolution, slightly unbalanced optical dispersion in the interferometer arms, and measurement errors that are accentuated in differentiating the phase response acquired by the VNA.

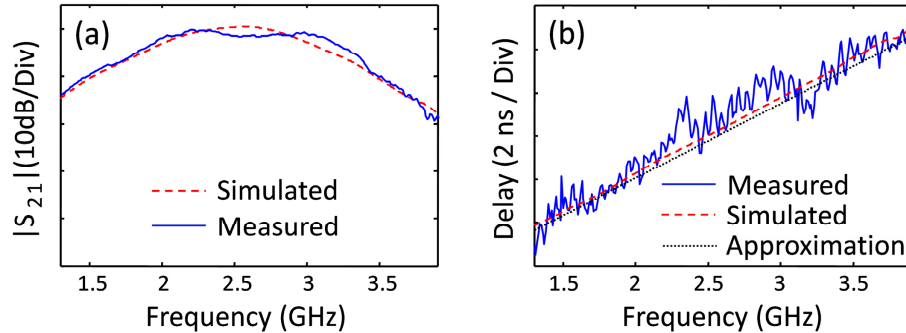


Fig. 3. (a) Measured (solid) and simulated (dashed) amplitude filter transfer functions of MWP phase filter on dB scale with a coefficient of quadratic phase $\beta = -0.017$ applied to the comb. (b) Group delay of the filter: measured (solid), simulated (dashed), and from approximate expression, Eq. (4) (dotted).

3. Microwave pulse compression

Next, we demonstrate the capability of the MWP phase filter to perform programmable spectral phase shaping in a pulse compression experiment whose layout is described in Fig. 4. We first generate a linearly chirped RF signal, synthesized by an arbitrary waveform generator (AWG) (Tektronix AWG 7122B) operating at 12 GS/s sampling rate. The chirped input signal is amplified and then connected to the MWP filter, which imposes the desired spectral phase function. The filtered output waveform is amplified and measured with a real-

time sampling scope (Tektronix DSA 72004B) with 20 GHz analog bandwidth and 50 GS/s sampling rate, which is triggered by the AWG's digital output.

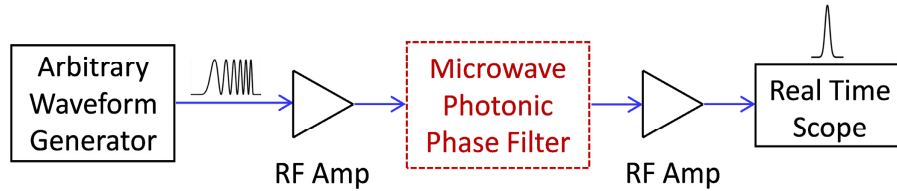


Fig. 4. Microwave pulse-compression experimental scheme.

Figures 5(a) show a linearly down-chirped input pulse generated by the AWG (left) and its corresponding RF spectrum (right), measured by the real-time sampling scope and RF spectrum analyzer, respectively, prior to the MPPF. The signal is programmed with a chirp coefficient of -3.7ns/GHz and $\sim 16\text{ ns}$ time aperture, repeating periodically every $\sim 20\text{ ns}$. The 160 optical taps lead to a maximum temporal aperture of $\sim 16\text{ ns}$. Its RF spectrum shows 2.7 GHz flat passband at -10 dB level and centered around 2.6 GHz. After sending the waveforms to the MPPFs with synthesized phase ($\beta = -0.017$), we compensate for the input chirp and obtain at the output the transform-limited waveforms illustrated in Fig. 5(b). One hundred traces of measured waveforms are averaged together to enhance the signal-to-noise ratio (SNR). The waveform (solid) is very close to the simulated result (dashed) as shown in Fig. 5(b) (left). The corresponding spectrogram (right) [28], for which we used a 0.4 ns Gaussian gating function, shows circle of contour lines without any slope, indicating compression very close to the bandwidth-limited duration. We also show a typical single-shot waveform in the inset of Fig. 5(b). Since the inherent fluctuations of the interferometer occur on a much longer time scale than either the temporal extension of the input waveform or the measurement time, the compressed signal shows a high SNR which may be further improved through averaging. To clearly illustrate the ability to reprogram the chirp coefficient of the MWP phase filter, we repeat the experiment with a linearly up-chirped input waveform with chirp coefficient $+3.7\text{ ns/GHz}$. The input waveform and its spectrum are shown in Fig. 5(c). As expected, both the temporal aperture (left) and RF spectrum (right) of the input waveform are very close to those shown in Fig. 5(a). We obtain best compensation for the input chirp by reprogramming the MWP phase filter using quadratic phase β equals to $+0.015$. As shown in Fig. 5(d), the compressed pulse is very similar to that obtained in Fig. 5(b) for the down-chirped input. The corresponding spectrogram is close to horizontal, again indicating high-quality (chirp-free) pulse compression.

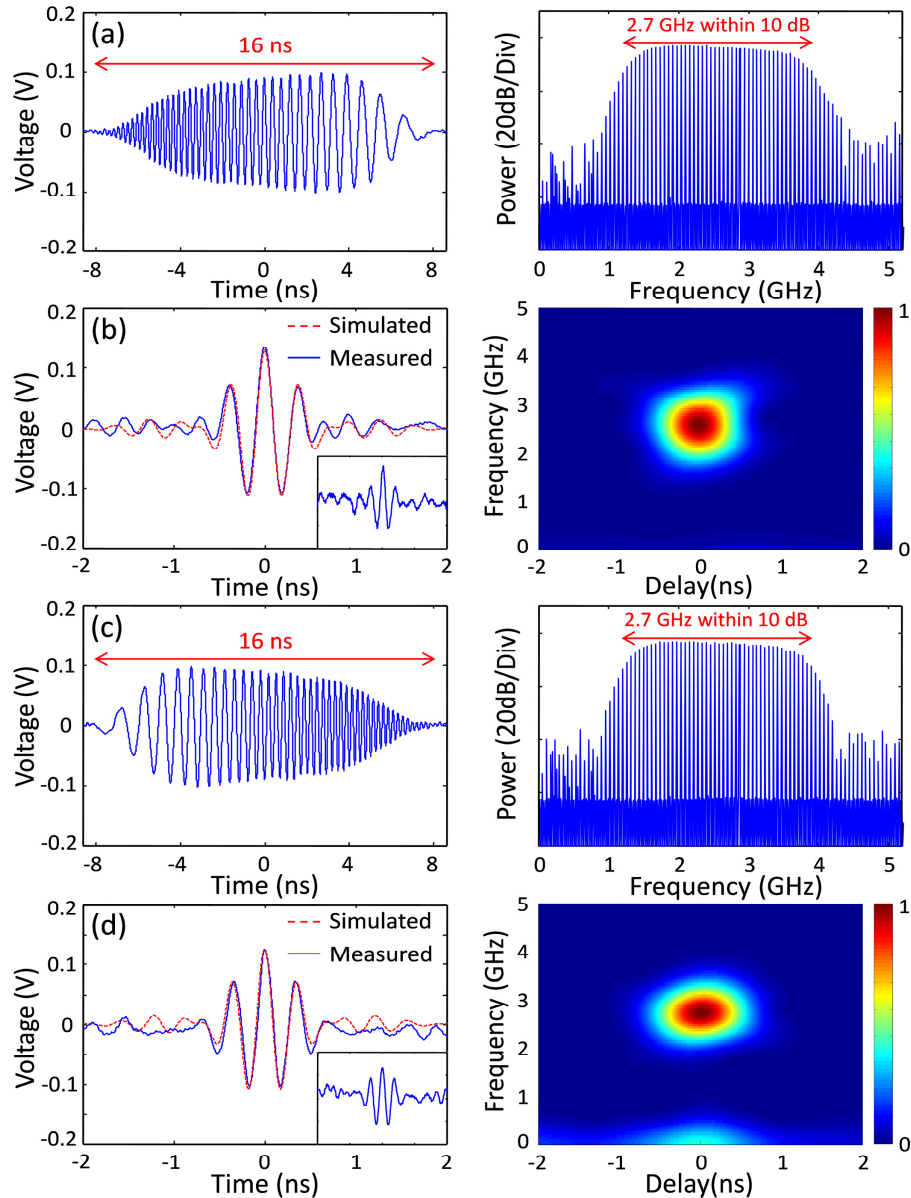


Fig. 5. Measurement results for phase-matched filtering. (a) (c) Temporal profiles of input linearly chirp pulses (left) and corresponding measured RF spectra of synthesized input pulses (right) with (a) -3.7 ns/GHz and (c) $+3.7$ ns/GHz chirp respectively, and (b) (d) corresponding compressed pulses (left) and their spectrograms (right) after matched filtering. Inset of (b) and (d), single-shot waveforms with same x and y axis scale as (b) and (d).

4. Conclusion

In summary, we have designed a MWP phase filter with ~ 160 programmable complex-coefficient taps. The scheme combines optical line-by-line shaping techniques with a 10 GHz ultrabroadband optical frequency comb generator as the light source. In our interferometric scheme, optical quadratic phase programmed in a line-by-line fashion enables control of filter dispersion in the ns/GHz regime. With this platform, we have shown the potential of this scheme for phase-matched filtering operation by compressing broadband microwave pulses

with ~ 16 ns temporal apertures. This study is to our knowledge the first to simultaneously achieve long time apertures and large TBWP in programmable and tunable RF phase filtering, compatible with the strong demands of modern ultrabroadband RF systems.

Acknowledgment

This work was supported in part by the Office of the Assistant Secretary of Defense for Research and Engineering under the National Security Science and Engineering Faculty Fellowship program through grant N00244-09-1-0068 from the Naval Postgraduate School. Any opinion, findings, and conclusions or recommendations expressed in this publication are those of the authors and do not necessarily reflect the views of the sponsors. We would like to thank Dr. Daniel E. Leaird for his technical assistance and valuable discussions.